Electronic structure, magnetism, and spin fluctuations in the superconducting weak ferromagnet Y_4Co_3

B. Wiendlocha,* J. Tobola, S. Kaprzyk, and A. Kolodziejczyk

Faculty of Physics and Applied Computer Science, AGH University of Science and Technology, Al. Mickiewicza 30, PL-30-059 Cracow, Poland

(Received 2 December 2010; revised manuscript received 25 January 2011; published 11 March 2011)

Results of the first principles study on the electronic structure and magnetism of the superconducting weak ferromagnet Y_4Co_3 are presented. Using the full potential Korringa-Kohn-Rostoker (FP-KKR) method, densities of states, dispersion curves, and magnetic moments were calculated for a quasiordered structural model of the compound in the framework of the local-density approximation. Spin-polarized KKR calculations confirm that weak ferromagnetic properties of Y_4Co_3 can be attributed to only one cobalt atom located on the (2b) site in the unit cell, while another 20 Co and Y atoms act as a diamagnetic environment. Moreover, the magnetic Co atoms form quasi-one-dimensional chains along the z direction. The magnitude of the Co(2b) magnetic moment (0.55 μ_B) markedly overestimates the experimental value (0.23 μ_B), which suggests the importance of spin fluctuations in this system. Calculated distribution of spin magnetization in the unit cell provides a background for discussion of the coexistence of ferromagnetism and superconductivity in Y_4Co_3. Finally, the effect of pressure on magnetism is discussed and compared with experimental data, also supporting weak ferromagnetic behaviors in the system.

DOI: 10.1103/PhysRevB.83.094408 PACS number(s): 74.25.Jb, 74.25.Ha, 75.10.Lp

I. INTRODUCTION

Unusual properties of Y_4Co_3, that is the coexistence of superconductivity and ferromagnetism, were observed 30 years ago.[1] The superconducting and ferromagnetic critical temperatures are about $T_s \sim 2.5$ K and $T_C \sim 4.5$ K, respectively. After this finding, the system was intensively studied using different techniques, since it was the first example where superconductivity coexisted with weak itinerant ferromagnetism, with both phenomena driven most likely by the d-band electrons. To our best knowledge, Y_4Co_3 is, up to now, a unique compound containing transition-metal elements only, where coexistence of ferromagnetism and superconductivity occurs, since other systems always contain f-like elements, e.g., UGe_2,[2] URhGe,[3] UCoGe,[4] or the recently discovered P-doped $EuFe_2As_2$.[5] Moreover, Y_4Co_3 was likely the first example, where superconductivity occurred below a transition to ferromagnetism, with both phenomena coexisted at least in the range between 1 K and 2.5 K.[6,7] This was another difference to previously known magnetic superconductors, e.g., $ErRh_4B_4$ or $HoMo_6S_8$ (see, Refs. 8–10), where magnetism appeared below T_s, suppressing superconductivity.

Although Y_4Co_3 has been known since 1980, the first principles study on its magnetism (e.g., calculations of magnetic moments) was not presented until now. We have found two papers reporting electronic structure of this system from *ab initio* calculations. An interesting discussion of electronic structure of related compound Y_9Co_7 based on non-spin-polarized computations can be found in Ref. 11 (for connections between Y_4Co_3 and Y_9Co_7, see below). A more recent paper, Ref. 12, briefly reports on the electronic structure calculations for Y_4Co_3, also in a nonmagnetic state.

As is worth noting, one may notice a renewed interest on this system due to very recent experimental investigations.[13]

In this paper the results of band-structure calculations for Y_4Co_3 are presented. We attempt to answer some open questions, e.g., whether the magnetism is an intrinsic property of the system or an effect of crystal imperfections,[11] or what is the microscopic reason for magnetism occurrence in Y_4Co_3. The implications of our electronic structure calculations on the current model of the coexistence of ferromagnetism and superconductivity in Y_4Co_3 are also discussed.

A. Review of the experimental data

In this section we summarize shortly crystal structure and magnetism data, available for Y_4Co_3. For a more complete review, see, e.g., Refs. 6 and 7. The crystal structure of the Y-Co system near 1 : 1.3 stoichiometry is rather complex, and was originally described in the hexagonal unit cell of the Ho_4Co_3 type[14] (Fig. 1). A unit cell can take 22 atoms, being distributed over three inequivalent Co sites and two inequivalent Y sites. All positions are gathered in Table I. As the unit cell includes three formula units, for the Y:Co stoichiometry equal to 4 : 3, the Co(2b) sites are half-filled (50%) and the number of atoms in the unit cell is equal to 21. Thus, in this crystallographic model, Y_4Co_3 cannot be regarded as an ordered compound, but as an disordered alloy with (2b) sites occupied randomly by cobalt [Co atom on (2b) site will be called Co(3)] and vacancies (Vac). Thus, the crystal cell of this alloy better corresponds to the formula $Y_{12}Co_{8+2x}$ with $x = 0.50$ than to the formula Y_4Co_3, suggesting an ordered system. The unit cell (Fig. 1) consists of the "separated" Co/Vac chains forming the cell edges and the Y(1)-Y(2)-Co(1)-Co(2) trigonal prisms filling most of the unit cell. The partial occupation of the Co(3) site is likely connected with a short distance between the neighboring (2b) positions (∼2Å).

In the 1980s, after revealing the coexistence of ferromagnetism and superconductivity in Y_4Co_3, the Ho_4Co_3-type unit cell appeared to be only an approximation for the real structure of the system. There was a debate whether this system should be called Y_9Co_7 (instead of Y_4Co_3), since it was found[6,7,15] that Y_9Co_7 (richer in cobalt) exhibited better superconducting properties (∼0.5 K higher T_s) than Y_4Co_3. It was even suggested, that Y_4Co_3 as a single phase compound might not exist.[15] Employing the initial notation, the 9 : 7 stoichiometry compound corresponds to $Y_4Co_{3.11}$, but one should bear in mind that for Y_9Co_7 an ordered model of structure was

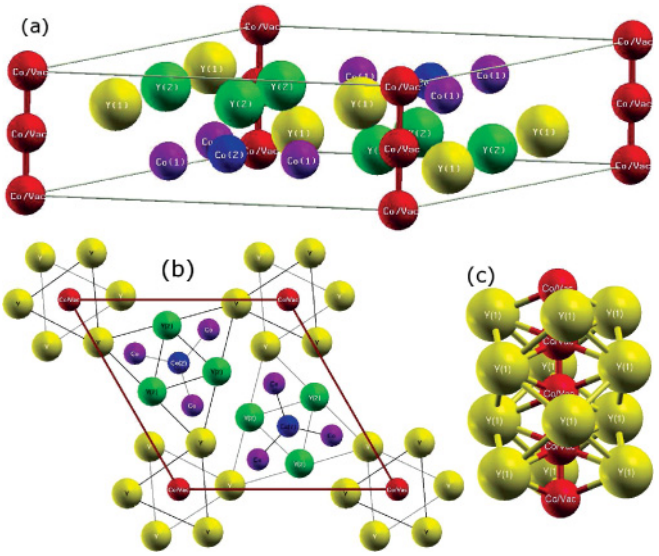

FIG. 1. (Color online) (a) Unit cell of Y_4Co_3 used in the calculations. The edges of the unit cell, i.e., (2b) sites, are occupied by cobalt or vacancy (Co/Vac), on average every second position is occupied by cobalt, called here Co(3). Atomic positions are presented in Table I. (b) The body of the unit cell is formed by the trigonal prisms of Y(1), Y(2), Co(1), and Co(2), the black lines and labels denotes atoms in the $z = 0.75$ plane, while white denotes $z = 0.25$ plane. (c) The in-plane triangles of Y(1) atoms form channels along z direction, surrounding the Co(3) atoms chains.

suggested[15] with the unit cell tripled along the c axis. In such a superstructure, the Co(3) atoms positions are adapted in such way to make the Y-Co system perfectly ordered for 9 : 7 composition (100% filling of all sites, see, e.g., Refs. 11 and 15 for details). The resulting crystal structure exhibits reduced symmetry, trigonal instead of hexagonal.[14] However, the ordered model of the superstructure was not confirmed by x-ray measurements on single crystal samples.[14] Moreover, it was also reported[14] that the Co(3) atoms did not occupy the fixed lattice positions, and were rather arranged in chains with undetermined period. Thus, the basic unit cell shown in Fig. 1 can be treated as the best established and simplest approximation of the real structure both for Y_4Co_3 and Y_9Co_7, as far as the Co(3) atoms location is concerned. The $Y_{12}Co_{8+2x}$ model represents the Y_4Co_3 and Y_9Co_7 compounds, when the Co(3) concentration reaches the values of $x = 0.50$ and $x = 0.66$, respectively. However, the question on the real unit cell of Y_4Co_3 and Y_9Co_7 and whether they describe the same crystal structure with various Co contents, is still open.

TABLE I. Atomic positions of the Y_4Co_3 compound (type Ho_4Co_3, space group No. 176, $P63/m$). Lattice parameters are:[16] $a = 11.527$ Å, $c = 4.052$ Å.

Atom	Site	Coordinates	x	y
Y(1)	(6h)	$(x,y,\frac{1}{4})$, $(\bar{y},x\text{-}y,\frac{1}{4})$ $(y\text{-}x,\bar{x},\frac{1}{4})$ $(\bar{x},\bar{y},\frac{3}{4})$ $(y,y\text{-}x,\frac{3}{4})$, $(x\text{-}y,x,\frac{3}{4})$	0.7543	0.9791
Y(2)	(6h)	as above	0.1360	0.5150
Co(1)	(6h)	as above	0.4415	0.1578
Co(2)	(2d)	$(\frac{2}{3},\frac{1}{3},\frac{1}{4})$, $(\frac{1}{3},\frac{2}{3},\frac{3}{4})$	–	–
Co(3)	(2b)[a]	$(0,0,0)$, $(0,0,\frac{1}{2})$	–	–

[a]In our calculations (2b) positions are split into (1a) (0,0,0) and (1b) $(0,0,\frac{1}{2})$, being occupied by Co and vacancy, respectively (see text).

In the present work, the basic unit cell, presented in Fig. 1, with $x = 0.50$ was employed to account for the Y_4Co_3 case. This crystal model has allowed us to use the full potential Korringa-Kohn-Rostoker code adapted to electronic structure calculations of ordered compounds (see Sec. II).

As far as the superconducting properties are concerned, it is generally believed, that superconductivity in Y_4Co_3 has a singlet-like character and probably mediated by the electron-phonon interactions.[6] The system exhibits all the characteristic features of conventional superconductors (see Refs. 6 and 7 and references therein), e.g., perfect diamagnetic Meissner state, the specific heat jump at T_s correlated with a drop in resistivity and susceptibility. More puzzling is the type of its magnetism. The system shows, e.g., a modified Curie-Weiss behavior, with susceptibility maximum[17] and specific heat jump near the Curie temperature,[18] suppression of magnetism with pressure,[19] and a hysteresis loop in the magnetization measurements[20] interpreted as fingerprints of a ferromagnetic state. There are different values of magnetization reported in literature. For the 4 : 3 composition one can find $M = 0.045\ \mu_B$/f.u. measured for the $Y_4Co_{3.03}$ sample[21] and extrapolated to $T = 0$ K or $M \simeq 0.03\ \mu_B$/(f.u. Y_4Co_3) at 1.24 K.[20] Note, that these values are not exact, firstly diamagnetism induced by superconductivity below 2.5 K does not allow to accurately measure bulk magnetization, and secondly it is difficult to measure magnetization in a weak ferromagnetic system.[21]

From the NMR measurements[22] it was found that there were three inequivalent Co sites in Y_4Co_3, but magnetism was attributed only to the cobalt atoms on the (2b) site. The estimated magnetic moment was $\mu_{Co(3)} = 0.23\,\mu_B$, and important spin fluctuations were observed. Actually, there are no other experimental papers on the determination of the Co(3) magnetic moment, thus our theoretical result is compared to this value. Most of the experimental results concerning the magnetism of the Y-Co system were interpreted in the framework of the spin-fluctuation theory of the weak-itinerant ferromagnetism,[23] showing characteristic features as, e.g., the zero-field magnetization $M(T)^2 \propto T^{4/3}$ (Ref. 21) or resistivity $\rho \propto T^2$ (Ref. 17). However, more exotic models without long-range ferromagnetic ordering were also considered, i.e., basing on the μSR measurements[24] the magnetic state of Y_9Co_7 was called "crypto-itinerant ferromagnet," some hybrid magnetic and superconducting states were suggested,[25] while short-range order was discussed elsewhere.[26]

On the whole, magnetic properties of the Y-Co system near 4 : 3 or 9 : 7 stoichiometry were found to be similar and weakly dependent on Y:Co composition[27] (comparing to superconducting behaviors), except for increasing magnetization with increasing Co content. (Magnetization measured for Y_9Co_7 sample and extrapolated to $T = 0$ K was $M \simeq 0.383$ emu/g, which referred to the 4 : 3 composition gives about $M = 0.10\,\mu_B$/(f.u. Y_4Co_3), and is higher than in Y_4Co_3 likely due to higher Co(3) atoms concentration.[28]) All these data allow to suppose that general conclusions deduced from the first principles calculations for Y_4Co_3 should also

be maintained for Y_9Co_7 (e.g., we may expect similar local magnetic moments). Also, some experimental results available only for Y_9Co_7 (e.g., effect of pressure on magnetism), should provide a reliable comparison with theoretical results obtained for the quasiordered model of Y_4Co_3.

To summarize this short review, the commonly accepted phenomenological model of the coexistence of superconductivity and magnetism in the Y_4Co_3/Y_9Co_7 system is as follows: There is an itinerant weak ferromagnetic state below T_C with the Co(3) sublattice responsible for magnetism, combined with superconductivity below T_s, being mostly attributed to the Y-Co triangular prisms inside the unit cell. Both physical phenomena visibly compete (e.g., external pressure suppresses magnetism and enhance superconductivity[19,29]), but their coexistence is possible due to some spatial "separation" of atom sublattices responsible for different phenomena.[6,7] However, this separation cannot be treated in the strict sense, since the Ginzburg-Landau coherence length was estimated to be as large as 300 Å (roughly 30 times larger than the unit cell size).[30] One can tentatively imagine this uncommon state as a "superconducting sea" with the Co(3) "magnetic islands" embedded. The question on the existence of the "magnetic islands" and whether Co(3) moments are ordered in Y_4Co_3 has not been yet addressed to first principles calculations. Hence, the KKR results presented here may help to enlighten this problem.

II. COMPUTATIONAL DETAILS

Electronic structure calculations were performed using the *full potential* Korringa-Kohn-Rostoker (FP-KKR) technique based on the Green function multiple scattering theory.[31–33] In our implementation of the FP-KKR method, the unit cell is divided into the set of generalized Voronoi polyhedrons arbitrary formed around inequivalent sites, that completely fill the Wigner-Seitz cell. The crystal potential has been constructed in the framework of the local spin-density approximation (LSDA), using the Perdew-Wang formula[34] for the exchange-correlation part. All results were carefully checked for the **k**-point number convergence, using more than 100 points in the irreducible part of the Brillouin zone for the tetrahedron integration method. The results of FP-KKR semirelativistic calculations are presented, with the fully relativistic treatment of core electron energy levels.

In this work, the ordered model of the hexagonal cell (Fig. 1) was used in the electronic structure calculations. To take into account the partial filling of the Co(2b) site in Y_4Co_3 in the KKR method, we employed a "quasi-disordered" structure, i.e., the (2b) position was split into two nonequivalent sites, (1a) and (1b). The (1a), i.e., (0,0,0) position, was occupied by a Co atom [Co(3)] and (1b), $(0,0,\frac{1}{2})$ site, by a vacancy (Vac), i.e., an empty sphere with $Z = 0$. This structural modification resulted in the lowering of the hexagonal cell symmetry from space group $P63/m$ (No. 173) to $P\text{-}3$ (No. 147), with reduction of symmetry operations from 12 to 6. As mentioned above, this model is admitted to consider the Y_4Co_3 composition only. It was verified by additional calculations that the KKR results remain unchanged when the positions of Co(3) and Vac were exchanged [cobalt on (1b) site and empty spheres on (1a) site], as one expects from equivalence of both sites in the proper space group.

III. RESULTS AND DISCUSSION

A. Non-spin-polarized electronic structure

The discussion of the electronic structure of Y_4Co_3 is started from an analysis of general features in the non-spin-polarized case. The total and site-decomposed electronic densities of states (DOS) are presented in Fig. 2. Due to the large number of atoms in the unit cell and, in consequence, various interatomic distances, the DOS has a complex shape. The Fermi level (E_F) is located in the DOS valley, which can tentatively support the chemical stability of this system. The valence band region is formed from the strongly hybridized atomic states of Co ($3d$, $4s$) and Y ($4d$, $5s$), with important $s-p$ and $s-d$ charge transfers. The Y-$4p$ states constitute the semicore level, located about -1.5 Ry below the Fermi level (not shown). Generally, the body of the electronic structure is dominated by contributions from the Y(1)-Y(2)-Co(1)-Co(2) block, which form the triangular prisms inside the unit cell (Fig. 1). Nominally, the major contribution to DOS comes from six Co(1) atoms, due to the highest number of valence electrons ($54e$) given to the bands. The single Co(3) atom, building the separated cobalt chains, roughly governs the position of the Fermi level due to DOS significantly different from other atoms (a high d-like peak below E_F), which enables the Co(3) to play an important role in the ground-state properties of Y_4Co_3.

To have a deeper insight into the influence of each atom on electronic structure, the site-decomposed DOS are plotted for inequivalent sites (Figs. 3 and 4). The most striking DOS feature of Y_4Co_3 is that, except for Co(3), the Fermi level is systematically placed in the local DOS valleys, resulting in relatively low total DOS. The calculated small DOS at E_F per atom (see Table II) would rather not suggest a transition to a ferromagnetic state. In contrast to other atoms, Co(3) exhibits apparently different DOS, due to a large d-like peak found just below the Fermi level (E_F is placed on the decreasing DOS slope). This feature yields the highest DOS value (per atom) for Co(3) in comparison to other contributions (Table II). Actually,

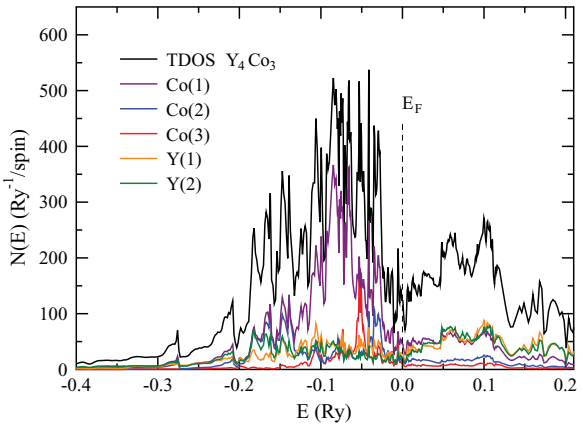

FIG. 2. (Color online) Total and site-decomposed densities of electronic states in Y_4Co_3 (per unit cell, i.e., three formula units), from non-spin-polarized calculations.

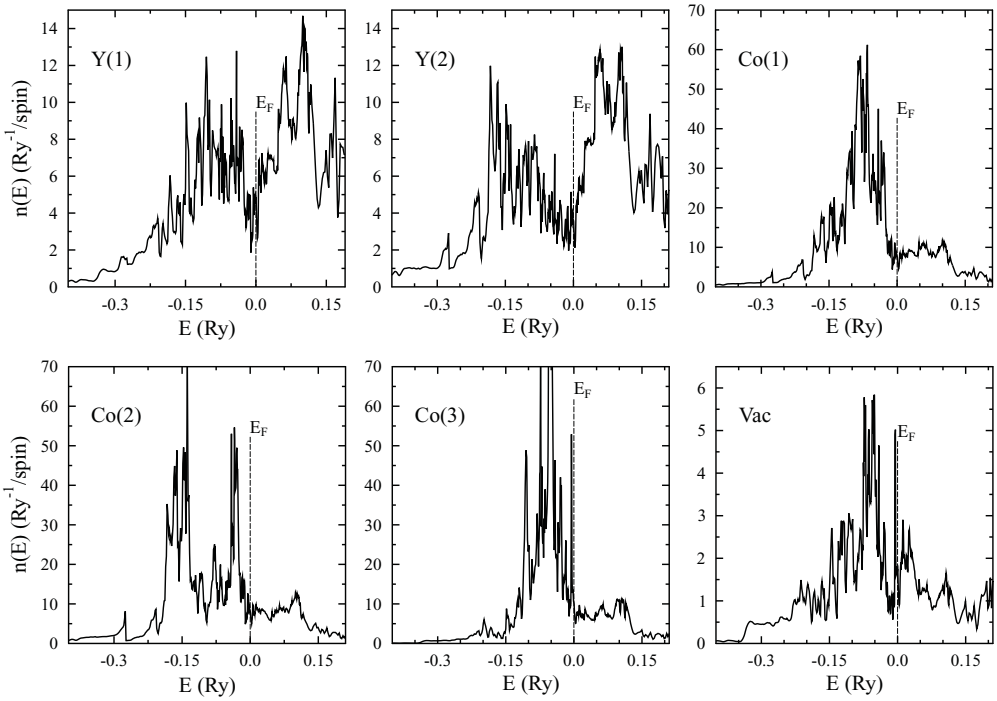

FIG. 3. Site-decomposed DOS per atom from non-spin-polarized calculations.

the value $n(E_F) \simeq 10$ Ry^{-1}/spin is too small to satisfy the Stoner criterion, since the calculated Stoner parameter for Co(3) atom $S = I_d n_d(E_F)$ is only about 0.6. Thus, the Stoner analysis based on non-spin-polarized DOS and the exchange integral predicts a nonmagnetic ground state of Y_4Co_3. However, the presence of a large and narrow DOS peak in the vicinity of E_F causes the simple Stoner criterion of ferromagnetism onset to be taken with care and accurate spin-polarized calculations may determine the preferred ground state.

B. Ferromagnetism

Indeed, the spin-polarized calculations do not confirm the nonmagnetic state deduced from the Stoner criterion. Figure 5 presents the spin-polarized DOS shape of Y_4Co_3. At first glance, the differences between the non-spin-polarized (Fig. 2) and spin-polarized (Fig. 5) total DOS are hardly visible, since spin-up and spin-down DOS functions are very similar. However, the spin-polarized KKR calculations finally resulted in a stable, ferromagnetic ground state. The partial, site-decomposed DOS (Fig. 5) show that only the Co(3) atom exhibits polarization in the DOS shape, as depicted in Fig. 4, being confirmed by the appearance of a local

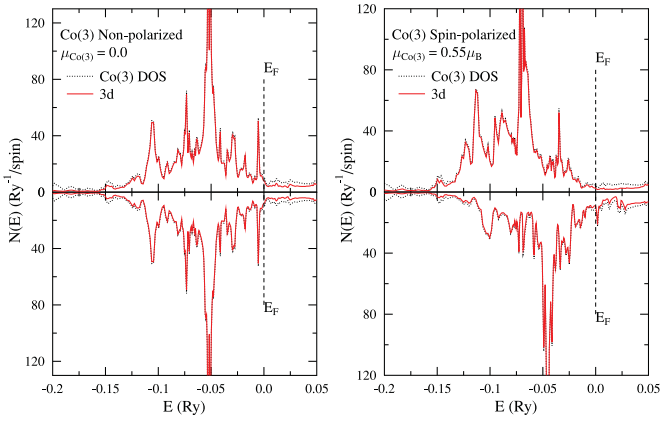

FIG. 4. (Color online) Comparison of the Co(3) partial DOS from non-spin-polarized (left) and spin-polarized (right) calculations. Peak under E_F in nonmagnetic state is well visible.

TABLE II. Electronic properties of Y_4Co_3. Values of DOS $n(E_F)$ are given in (Ry^{-1}/spin), magnetic moments μ in (μ_B), S stands for the Stoner parameter.

Non-spin-polarized calculations			
Atom	$n(E_F)$	$n_d(E_F)$	S
Y(1)	3.62	2.50	0.15
Y(2)	4.85	3.37	0.19
Co(1)	7.71	5.79	0.43
Co(2)	8.00	6.86	0.48
Co(3)	10.31	8.19	0.61
Vac	1.73	0.47	–
$N(E_F) = 250$ Ry^{-1} per unit cell			

Spin-polarized calculations					
Atom	$n_\uparrow(E_F)$	$n_\downarrow(E_F)$	$n_{\uparrow d}(E_F)$	$n_{\downarrow d}(E_F)$	μ
Y(1)	4.00	4.22	2.72	2.91	−0.024
Y(2)	2.90	4.02	1.96	2.92	0.004
Co(1)	6.37	7.18	4.83	5.18	−0.007
Co(2)	6.45	7.38	5.49	6.41	−0.017
Co(3)	4.26	10.75	2.37	9.14	0.551
Vac	1.07	1.15	0.39	0.37	0.016
$N_\uparrow(E_F) = 99$ Ry^{-1} $N_\downarrow(E_F) = 120$ Ry^{-1}					

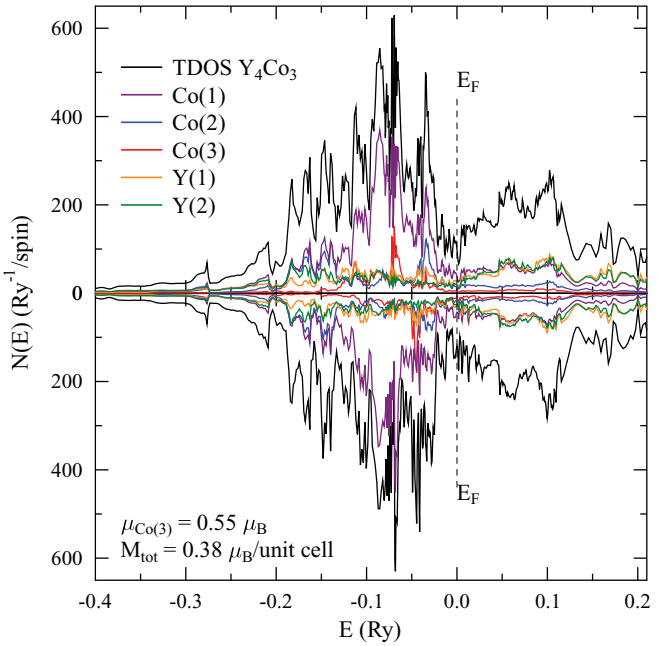

FIG. 5. (Color online) Total and site-decomposed densities of electronic states in Y_4Co_3 from spin-polarized calculations.

magnetic moment (Table II). The Co(3) magnetic moment of about $\mu_{Co_3} = 0.55\ \mu_B$ decides in favor of magnetism in Y_4Co_3, since the remaining atoms possess small magnetic moments ($\leqslant 0.02\,\mu_B$). Such small DOS polarizations seen on other atoms should be considered rather as a response to the magnetic field of the Co(3) atom, than intrinsic local magnetic moments. The total magnetization $M_{tot} = 0.38\,\mu_B$/unit cell yields $M \simeq 0.13\,\mu_B$ per Y_4Co_3 formula unit. M_{tot} is lower than μ_{Co_3} due to the overall "diamagnetic" response of the Y-Co triangular prisms, generating about $-0.1\,\mu_B$. The comparison with the experimental values is discussed in Sec. III D.

The specific character of the Y_4Co_3 electronic structure can be observed in the electron dispersion curves, shown in the Fig. 6. In the Γ-M-K-Γ triangle no band crosses the Fermi level for both spin directions, and this behavior holds for any direction in the $k_z = 0$ plane, as was checked by extensive calculations along randomly chosen directions. A similar result was earlier observed from non-spin-polarized calculations.[12] The ferromagnetic state leads mainly to the slight shift of dispersion curves and some changes in details. Since, the Y_4Co_3 system is predicted to possess an energy band gap in the $k_z = 0$ plane, it would be interesting to verify it (likely detectable on the ARUPS spectra, but due to the lack of single crystals there are no such results available). The vanishing Fermi surface in the $k_z = 0$ plane is presumably responsible for the DOS valley formed around E_F (Fig. 5). In the Γ-A direction (along the k_z axis), almost linear and strongly dispersive bands cross E_F, while in the A-L-H-A triangle, which is just a shift of the Γ-M-K-Γ triangle to the Brillouin zone top, bands crossing E_F become flat, which mostly gives rise to metallic-like properties of Y_4Co_3.

On the whole, the important result from presented spin-polarized KKR calculations concerns the fact that there is no need to search for an unconventional mechanism to explain magnetism in the Y_4Co_3 system. The energetically unfavorable DOS peak just below E_F (Fig. 4) on the single Co(3) atom, seems to be the reason for turning the system into the ferromagnetic state. In the magnetic state, the spin-up peak is not seen near E_F, while in the spin-down DOS the peak is smaller and is expelled above E_F. In Ref. 11, devoted to the electronic structure and magnetism of Y_9Co_7, the authors suggested two models of magnetism of this system, called A and B. Briefly, in model A magnetism was attributed to the excess Co atoms on Y(1) and Y(2) sites, while in model B the magnetism came from itinerant electrons of Co on (2b) sites. The authors[11] did not definitely conclude, which model was valid, but model A was said to be the most probable, and the "perfect Y_9Co_7 crystal" was expected to be paramagnetic. From our results we see that itinerant ferromagnetism is an intrinsic property of the Y_4Co_3 system. Hence, additional defects as the excess Co atoms on Y sites are not necessary to give rise to ferromagnetism, even if instead of a long-range order in real material a short-range order appears, as suggested, e.g., in Ref. 26. Similar behavior is expected to be valid for Y_9Co_7, since as we mentioned in the Introduction, experimentally the magnetic properties of the Y-Co system do not change much between Y_4Co_3 and Y_9Co_7.[27]

To look closer at the magnetism of the Co(3) atom we can calculate the spin dependence of d-orbital occupation (actually, the diagonal elements of occupation matrix calculated using the imaginary part of the Green's function, defined as $\langle l_1 m_1| -\frac{1}{\pi}\mathrm{Im}G|l_2 m_2\rangle$). The Co(3) (2b) site, being surrounded by Y(1) triangles in $z = \pm\frac{1}{4}$ planes, has a trigonal, C_{3i}

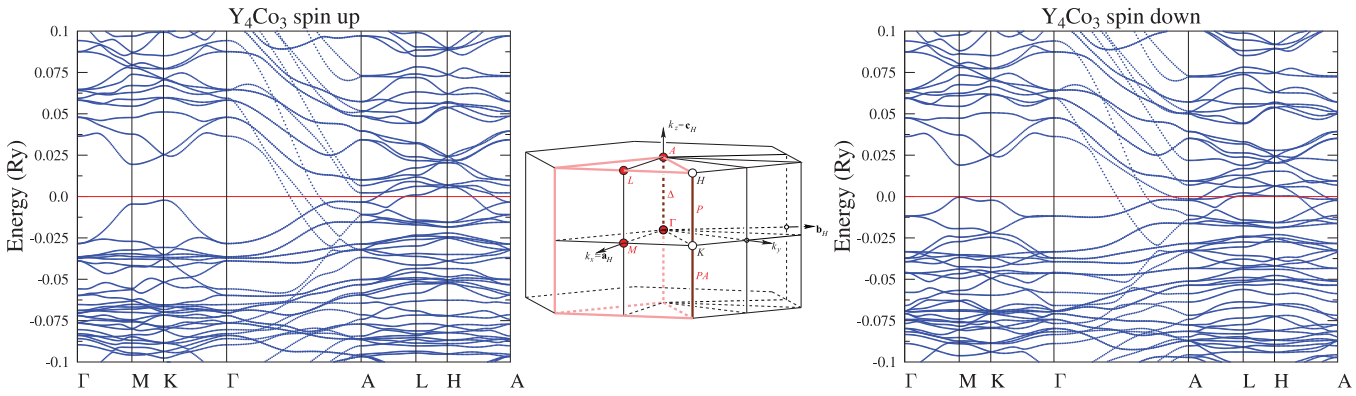

FIG. 6. (Color online) Electronic dispersion curves, $E_F = 0$. Center: Brillouin zone with the high symmetry points.[35,36]

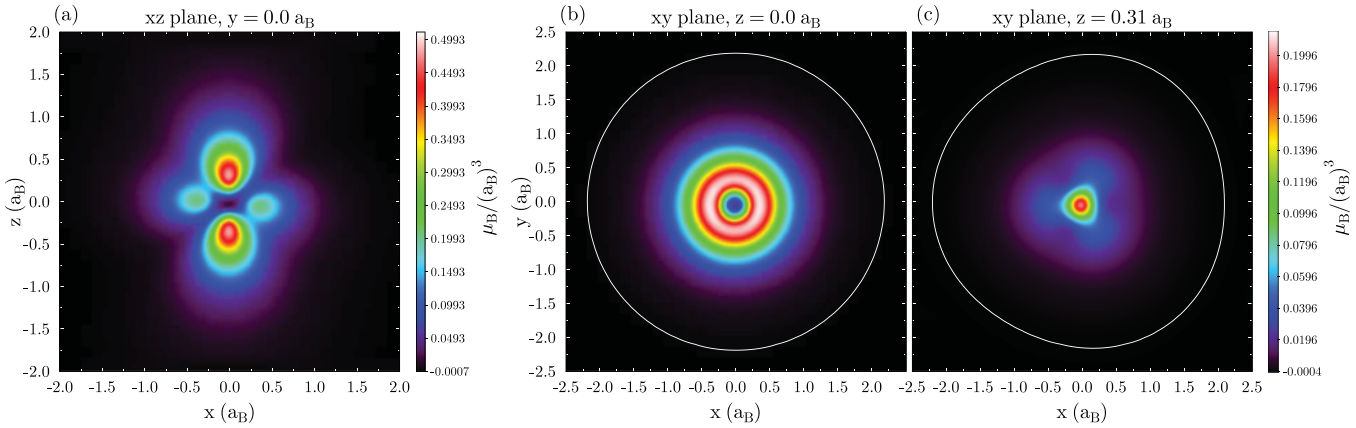

FIG. 7. (Color online) Spin-magnetization distribution in the (a) $y = 0$, (b) $z = 0$, and (c) $z = 0.04c$ (i.e., 0.31 a_B) planes.

symmetry. Thus, there are two degenerated E_g doublets, $\{d_{xy}, d_{x^2-y^2}\}$ and $\{d_{yz}, d_{xz}\}$ with occupation for both doublets approximately equal to $0.81e_\uparrow$ and $0.76e_\downarrow$. The d_{z^2} orbital (A_g representation, $l = 2, m = 0$), aligned in the z direction, is the highest-energy and least occupied orbital. It also has the highest level of polarization, with $0.79e_\uparrow$ and $0.49e_\downarrow$. Hence, about 60% of the magnetization comes from the d_{z^2} orbital and microscopically it is the main source of magnetism in this compound. The directional character of this orbital favors the simple ferromagnetic ordering of magnetic moments along the z axis.

The fact that the magnetic moments are "localized" only on Co(3) atoms can be well visualized on the spin-magnetization contour maps, presented in Figs. 7 and 8. The spin magnetization is calculated as a difference between the spin-up and spin-down electron densities. The magnetic moments reside on the Co(3) corner atoms, while the rest of the presented xz plane has magnetization close to zero (Fig. 8). The shape of magnetization around the Co(3) atom in the xz plane [Fig. 7(a)] confirms that the $3d_{z^2}$ orbital plays a major role in the constitution of the magnetic state. The xy cross sections well reflect the local symmetry of the magnetization, which should be trigonal (C_{3i}). Interestingly, in the $z = 0$ plane we may have an impression of cylindrical symmetry [Fig. 7(b)], due to the equally distanced Y(1) triangles ($z = \pm\frac{1}{4}$), each rotated by 60°. But, when we move off the $z = 0$ plane, triangle symmetry occurs [Fig. 7(c)].

Magnetism in Y_4Co_3 appears to be unusual. There is only one "magnetic atom" in the complex unit cell, and 20 other atoms form a diamagnetically polarized background. The

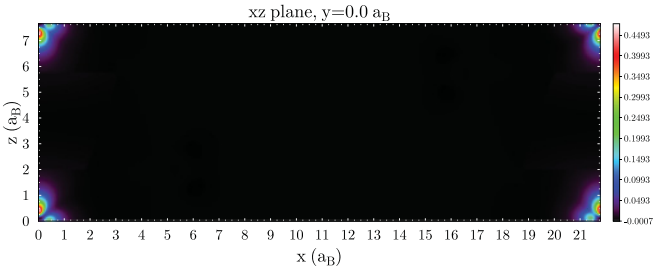

FIG. 8. (Color online) Spin-magnetization distribution in the $y = 0$ plane (face of the unit cell), showing that the charge density in the large areas of the unit cell is almost not polarized.

reason why other Co atoms are nonmagnetic is understood from non-spin-polarized partial DOS, where only the Co(3) atom exhibits an unstable DOS function due to the pronounced peak near E_F, while for Co(1) and Co(2) E_F is located in the DOS minimum. Inducing magnetic moments on the Co(1) and Co(2) atoms would make the system energetically unfavorable.

Another peculiarity of this crystal structure is the arrangement of Co(3) atoms in chains, lying in channels formed by the octahedras of Y(1) atoms (see Fig. 1). Thus, the Co(3) atoms form a quasi-one-dimensional magnetic structure, a feature which was announced for this system[26,29] but not explored in the past. This low dimensionality raises the question of whether the long-range ferromagnetic order can occur here, as the Mermin-Wagner theorem[37] predicts the lack of long-range magnetic order within a Heisenberg model with short-range interactions in one dimension. This of course does not completely rule out the presence of magnetic ordering for the three-dimensional structures with quasi-one-dimensional chains, but the properties of such systems are affected by the low-dimensional character. Recently, the quasi-one-dimensional ferromagnetism was investigated in some cobalt-based systems, like monoatomic Co chains on a Pt substrate[38] or Co oxides, like $BaCoO_3$ or $Ca_3Co_2O_6$ (see, e.g., Refs. 39–41). It is interesting to underline some structural similarities between Y_4Co_3 and aforementioned Co oxides. The Co(3) chains surrounded by Y(1) triangles, forming octahedras in the z direction, are similar to CoO_6 octahedras in the oxides family. In both cases, the chains are running along the c axis of the hexagonal cell. The geometrical difference is that in Y_4Co_3 the intra- and interchain Co-Co distances are about twice as large as in the oxides. The large interchain distance in Y_4Co_3 (11.5 Å) rather excludes the importance of the interchain magnetic interaction, which is of great importance in oxides, and leads to two-dimensional antiferromagnetic effects.[40] This quasi-one-dimensional character of magnetism in Y_4Co_3 makes this system even more interesting and opens new areas for future investigation.

C. Ferromagnetism vs superconductivity

The fact that most of the unit cell volume of Y_4Co_3 has negligible magnetization allows to draw some qualitative conclusions on the possibility of the coexistence of ferromagnetism and superconductivity. For example, in the xz cross

section of the unit cell, presented in Fig. 8, about 90% of the area has magnetization lower than $10^{-3}\ \mu_B/a_B^3$. For the whole unit cell, only 1.3% of the volume has a magnetization higher than $10^{-3}\ \mu_B/a_B^3$. Roughly speaking, if the electron density inside the unit cell has negligible polarization, in principle it cannot disturb forming singlet Cooper pairs. Certainly, the Cooper pairing acts in momentum space, so we should generally verify whether there are $(\mathbf{k}_\uparrow, -\mathbf{k}_\downarrow)$ electrons near the Fermi level. Since the $(\mathbf{k}, -\mathbf{k})$ degeneracy is ensured by the centrosymmetry of the unit cell, we should look for the $(\mathbf{k}_\uparrow, \mathbf{k}_\downarrow)$ states. From the band structure plot, e.g., in the Γ-A direction we observe three bands crossing E_F. Two of these bands are almost the same for both spin directions and they cross E_F in points: $\mathbf{k}_\uparrow = (0,0,0.2308)\frac{2\pi}{c}$, $\mathbf{k}_\downarrow = (0,0,0.2307)\frac{2\pi}{c}$, and $\mathbf{k}_\uparrow = (0,0,0.3422)\frac{2\pi}{c}$, $\mathbf{k}_\downarrow = (0,0,0.3410)\frac{2\pi}{c}$. These bands are mostly of the Co(1) and Y(2) character. So, one concludes that, in principle, there are electrons in the Y-Co trigonal prisms, which can form Cooper pairs and lead to singlet superconductivity. But more quantitative analysis of electron-phonon coupling is required to assess whether the BCS-type superconductivity can appear in Y_4Co_3.

Nevertheless, our results and conclusions may support the model of the coexistence of weak ferromagnetism and superconductivity in Y_4Co_3, with the ferromagnetism carried by chains of Co(3) atoms, screened by superconducting trigonal prisms of Y(1)-Co(1)-Y(2)-Co(2). Interestingly, this picture is qualitatively similar to the vortex lattice in type-II superconductors, since in both cases we have a superconducting sample penetrated by the magnetic-field lines, forming a hexagonal lattice.

D. Spin fluctuations

The calculated value of Y_4Co_3 magnetization [0.13 μ_B/(f.u.)], if compared to the measured $M = 0.045\ \mu_B$/(f.u.) is about 2.5 times overestimated. Similarly, comparing the calculated Co(3) magnetic moment $\mu_{Co_3} = 0.55\ \mu_B$ with the NMR estimation[22] $\mu_{Co_3} = 0.23\ \mu_B$ we get 2.5 times overestimation. This shows that Y_4Co_3 can be a rare example of the weak ferromagnetic system, where LDA tends to overestimate the tendency to magnetism, and suggests that it may be near the ferromagnetic quantum critical point.[42] The well-known similar examples are $ZrZn_2$ Sc_3In and Ni_3Al/Ni_3Ga (see, e.g., Refs. 43–46), where, due to strong spin fluctuations appearing in real samples, measured magnetic moments are much smaller than LDA (or GGA) values. Thus, our KKR-LDA results strongly support the classification of Y_4Co_3 as a weak itinerant ferromagnet with spin-fluctuation effects, as already suggested, basing on the analysis of experimental results.[17] In Y_4Co_3, an overestimation of the magnetic moment is a little smaller, compared to the aforementioned cases, since in hexagonal Sc_3In the LDA magnetic moment $\mu_{Sc} \simeq 0.35\ \mu_B$ is about 7 times higher than the experimental one,[33,44] while a factor of about 3 is established in $ZrZn_2$ (Ref. 43) and Ni_3Al (Ref. 46). This suggests that the spin fluctuations in Y_4Co_3 should be comparably weaker. The spin-fluctuations strength parameter λ_{sf}, which can be treated as the analog of the electron-phonon coupling constant λ_{ph}, can be extracted from the electronic specific-heat coefficient γ. The experimental value lies in the range of $\gamma \simeq 3.1$–3.4 mJ/(mol at. K^2).[18,47,48] Using the KKR-LDA value of total DOS at the Fermi level (spin-polarized case), $N(E_F) = 229$ Ry^{-1}, we get $\gamma_{LDA} = 1.89$ (mJ/mol at. K^2). Assuming that the band value is renormalized by the electron-phonon as well as the electron-paramagnon interaction (spin fluctuations), the formula $\gamma = \gamma_{LDA}(1 + \lambda_{ph} + \lambda_{sf})$, gives $\lambda_{ph} + \lambda_{sf} = 0.6$–$0.8$. This allows to safely put the upper limit $\lambda_{ph} + \lambda_{sf} < 1$. It is possible to have independent estimation of λ_{ph} and λ_{sf}, if one admits that superconductivity is driven by phonons and the McMillan formula,[49] can be applied here. We use the experimental value of T_s and the renormalized McMillan formula to take into account the spin fluctuations[50] (see, also Ref. 51 and references therein):

$$T_c = \frac{\Theta_D}{1.45}\ \exp\left\{-\frac{1.04(1+\lambda_{\text{eff}})}{\lambda_{\text{eff}} - \mu_{\text{eff}}^{\star}(1+0.62\lambda_{\text{eff}})}\right\}, \qquad (1)$$

with the renormalization:

$$\lambda_{\text{eff}} = \lambda_{\text{ph}}/(1+\lambda_{\text{sf}})$$
$$\mu_{\text{eff}}^{\star} = (\mu^{\star} + \lambda_{\text{sf}})/(1+\lambda_{\text{sf}}). \qquad (2)$$

The experimental Debye temperature is $\Theta_D \simeq 215$ K.[18] It is worth noting that the strong renormalization of Coulomb pseudopotential parameter $\mu^{\star}$ restricts the possible range of λ_{sf}, e.g., we can get $T_s \simeq 2.5$ K for $\lambda_{sf} = 0.1, \lambda_{ph} = 0.7$, and $\mu^{\star} = 0.08$ (yielding $\mu_{\text{eff}}^{\star} = 0.164$ and $\lambda_{ph} + \lambda_{sf} = 0.8$) or for $\lambda_{sf} = 0.15, \lambda_{ph} = 0.85$ ($\mu_{\text{eff}}^{\star} = 0.20$ and $\lambda_{ph} + \lambda_{sf} = 1.0$). Thus, we can estimate the electron-paramagnon interaction parameter to be of the order of $\lambda_{sf} \sim 0.1$, but rather not higher than 0.2. This qualitative discussion shows that the spin fluctuations are likely present in Y_4Co_3, but they are not as strong as, e.g., in Sc_3In, where $\lambda_{sf} > 1$ can be deduced from the specific-heat measurements in the magnetic field.[52,53] It is worth noting that similar measurements, i.e., the influence of high-magnetic field on the electronic specific heat, would be very helpful to study the presence and strength of spin fluctuations in Y_4Co_3.

E. Effect of pressure

The effect of pressure on the magnetic properties of Y_4Co_3 was also analyzed. We have performed calculations

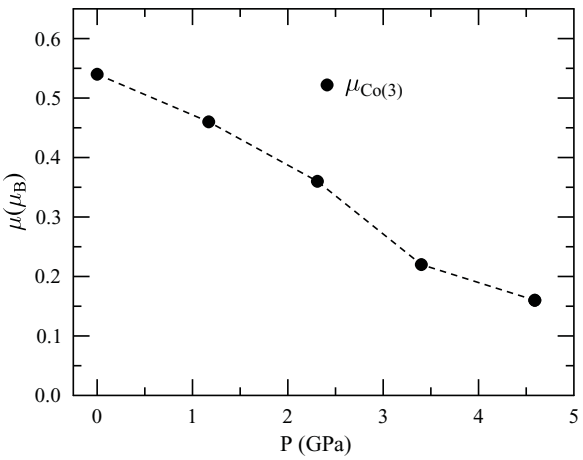

FIG. 9. Evolution of the Co(3) magnetic moment with pressure.

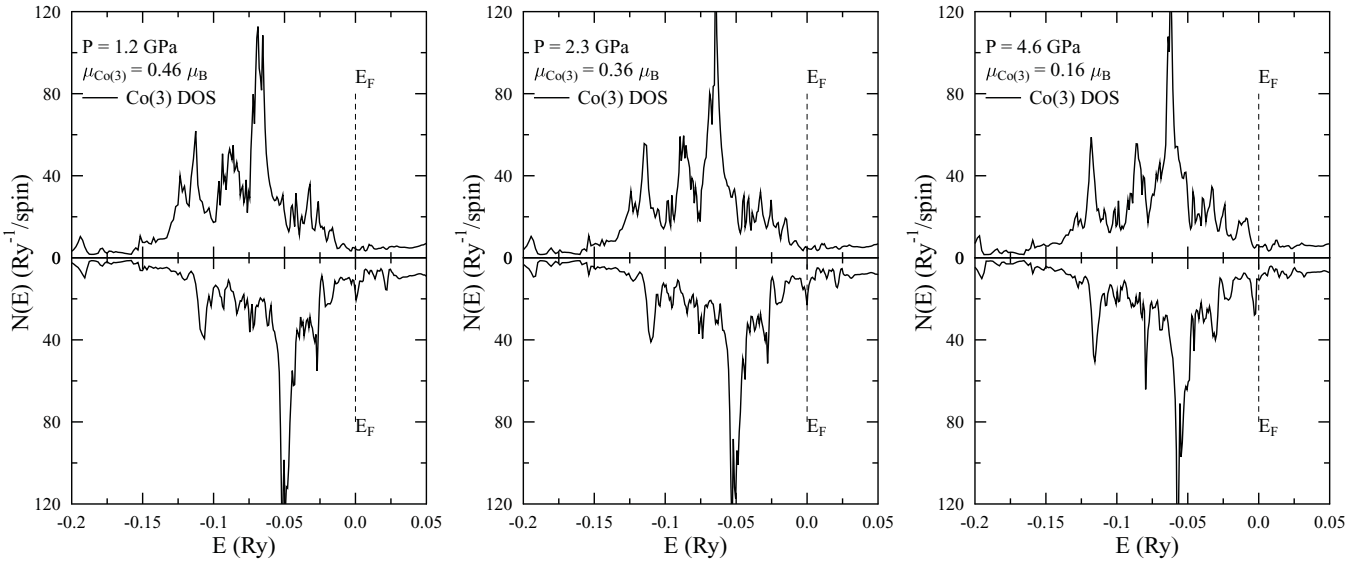

FIG. 10. Evolution of the Co(3) DOS with pressure. Peak under E_F is being formed.

under "quasi-hydrostatic" conditions. The a and c parameters were equally contracted in the range 0%–2% and all self-consistent calculations were started from the beginning. The bulk modulus, estimated under these conditions, is about $B = 75 \pm 5$ GPa, which is higher than the bulk modulus of yttrium (∼40 GPa[54]) and much smaller than the corresponding value for cobalt (∼200 GPa[55]). In calculations for the smaller unit cell volume, the magnetism is suppressed and the magnetic moment decreases rapidly, with the slope $\frac{\partial \mu}{\partial P} \simeq 0.08\ \mu_B$/GPa, as seen in Fig. 9. The reason for such behavior can be apparently seen from the evolution of the partial Co(3) DOS under pressure (Fig. 10). When the unit cell volume decreases, the spin-up DOS peak under E_F is being formed, while the spin-down peak, expelled above E_F in magnetic state, tends to move below E_F. Thus, the pressure lowers the DOS polarization and the magnetic moment, which additionally confirms that the Co(3)-DOS peak is responsible for the appearance of the magnetic moment on cobalt atoms on (2b) sites.

The suppression of magnetism under pressure from KKR calculations remains in agreement with the experimental trends observed in Y_9Co_7 (e.g., lowering of Curie temperature and magnetization,[19,29] for Y_4Co_3 there are no such results available in the literature). Extrapolation of the curve from Fig. 9 to zero magnetic moment gives the critical pressure, where magnetism completely disappears, as $p_c \simeq 7$ GPa. This value can be compared with very recent measurements of Y_9Co_7 under pressure,[13] where the critical pressure was estimated to be $p_c \simeq 3$ GPa. The overestimation of the critical pressure is in line with the spin fluctuations and weak ferromagnetism in this system, as revealed from our calculations. Interestingly, if the zero-pressure value of the magnetic moment, the NMR experimental estimation $\mu(Co_3) \sim 0.23\ \mu_B$, is accounted for, the theoretical slope $\frac{\partial \mu}{\partial P} \simeq 0.08\ \mu_B$/GPa also predicts a decrease of μ to zero for $p \simeq 3$ GPa.

IV. SUMMARY AND CONCLUSIONS

The results of the FP-KKR electronic structure calculations for the Y_4Co_3 system were presented. The ferromagnetic state obtained from spin-polarized computations can be attributed to the single Co atom located on the (2b) site, being the only magnetic atom among 21 in the unit cell, and forming quasi-one-dimensional magnetic chains. The LDA values of the magnetization ($M \simeq 0.13\ \mu_B$/f.u.), Co(3) magnetic moment ($\mu \simeq 0.55\ \mu_B$), and critical pressure ($p_c \simeq 7$ GPa) are overestimated compared with experiments, which can be tentatively explained in terms of weak ferromagnetism with moderate spin fluctuations ($\lambda_{sf} \sim 0.1$). The calculated spin-magnetization distribution, as well as other band structure parameters, leads to the conclusion that the conventional, singlet-like superconductivity may coexist with ferromagnetism in Y_4Co_3, due to relatively weak magnetic moments arranged along thin chains (the unit cell edges) on the one hand, and the presence of nonpolarized electrons at the Fermi level (filling most of the unit cell) on the other hand. On the whole, the FP-KKR results confirmed that the quasi-one-dimensional magnetism is an intrinsic property of Y_4Co_3 and its coexistence with singlet superconductivity may be possible.

ACKNOWLEDGMENTS

This work was partly supported by the COST P19 action and the Polish Ministry of Science and Higher Education (44/N-COST/2007/0).

*bartekw@fatcat.ftj.agh.edu.pl

[1] A. Kolodziejczyk, B. V. B. Sarkissian, and B. R. Coles, J. Phys. F **10**, L333 (1980).

[2] S. S. Saxena, P. Agarwal, K. Ahilan, F. M. Grosche, R. K. W. Haselwimmer, M. J. Steiner, E. Pugh, I. R. Walker, S. R. Julian, P. Monthoux *et al.*, Nature (London) **406**, 587 (2000).

[3]D. Aoki, A. Huxley, E. Ressouche, D. Braithwaite, J. Flouquet, J.-P. Brison, E. Lhotel, and C. Paulsen, Nature (London) **413**, 613 (2001).
[4]N. T. Huy, A. Gasparini, D. E. de Nijs, Y. Huang, J. C. P. Klaasse, T. Gortenmulder, A. de Visser, A. Hamann, T. Görlach, and H. v. Löhneysen, Phys. Rev. Lett. **99**, 067006 (2007).
[5]Z. Ren, Q. Tao, S. Jiang, C. Feng, C. Wang, J. Dai, G. Cao, and Z. Xu, Phys. Rev. Lett. **102**, 137002 (2009).
[6]A. Kolodziejczyk, IEEE/CSC & ESAS European Superconductivity news forum **1**, CR1 (2007) [http://ewh.ieee.org/tc/csc/europe/newsforum/pdf/Kolodziejczyk_Y9Co7_final_062707.pdf].
[7]A. Kolodziejczyk, B. Wiendlocha, R. Zalecki, J. Tobola, and S. Kaprzyk, Acta Phys. Pol. **111**, 513 (2007) [http://przyrbwn.icm.edu.pl/APP/PDF/111/a111z410.pdf].
[8]W. A. Fertig, D. C. Johnston, L. E. DeLong, R. W. McCallum, M. B. Maple, and B. T. Matthias, Phys. Rev. Lett. **38**, 987 (1977).
[9]J. Lynn, Solid State Commun. **26**, 493 (1978).
[10]M. Ishikawa and O. Fischer, Solid State Commun. **23**, 37 (1977).
[11]M. Shimizu, A. Kunihara, and J. Inoue, J. Phys. F **16**, 1263 (1986).
[12]T. Jeong, Solid State Commun. **138**, 261 (2006).
[13]T. Klimczuk, V. Sidorov, T. M. McQueen, F. Ronning, D. Safarik, J. D. Thompson, and R. J. Cava, *XIV Conference National School on Superconductivity, Ostrow Wielkopolski, Poland* (13-17.10.2009), [http://www.ifmpan.poznan.pl/ksn14/files/abstract_100.pdf].
[14]K. Yvon, H. F. Braun, and E. Gratz, J. Phys. F **13**, L131 (1983).
[15]B. V. B. Sarkissian, A. K. Grover, and B. R. Coles, Physica B+C **109–110**, 2041 (1982).
[16]A. Kolodziejczyk, J. Leciejewicz, A. Szytula, J. Chmist, and J. Wegrzyn, Acta Phys. Pol. A **72**, 319 (1987).
[17]A. Kolodziejczyk and J. Spalek, J. Phys. F **14**, 1277 (1984).
[18]A. Lewicki, Z. Tarnawski, C. Kapusta, A. Kolodziejczyk, H. Figiel, J. Chmist, Z. Lalowicz, and L. Sniadower, J. Magn. Magn. Mater. **36**, 297 (1983).
[19]C. Huang, C. Olsen, W. Fuller, J. Huang, and S. Wolf, Solid State Commun. **45**, 795 (1983).
[20]E. Gratz, J. O. Strom-Olsen, and M. J. Zuckermann, Solid State Commun. **40**, 833 (1981).
[21]Y. Yamaguchi, Y. Nishihara, and S. Ogawa, J. Magn. Magn. Mater. **31**, 513 (1983).
[22]M. Takigawa, H. Yasuoka, Y. Yamaguchi, and S. Ogawa, J. Phys. Soc. Jpn. **52**, 3318 (1983).
[23]T. Moriya, *Spin Fluctuations in Itinerant Electron Magnetism* (Springer-Verlag, Berlin, 1985).
[24]E. Ansaldo, Solid State Commun. **55**, 193 (1985).
[25]B. V. B. Sarkissian and A. K. Grover, J. Phys. F **12**, L107 (1982).
[26]A. K. Rastogi and B. R. Coles, J. Phys. F **15**, 1165 (1985).
[27]A. van der Liet, P. H. Frings, A. Menovsky, J. J. M. Franse, J. A. Mydosh, and G. J. Nieuwenhuys, J. Phys. F **12**, L153 (1982).
[28]A. Kolodziejczyk and C. Sulkowski, J. Phys. F **15**, 1151 (1985).
[29]B. V. B. Sarkissian and J. Beille, J. Appl. Phys. **55**, 2004 (1984).
[30]A. Kolodziejczyk and C. Sulkowski, in *Proceedings of the Low Temperature Conference LT-17, Karlsruhe*, edited by U. Eckern, A. Schmid, W. Weber, and H. Wühl (North-Holland, Amsterdam, 1984).
[31]A. Bansil, S. Kaprzyk, P. E. Mijnarends, and J. Toboła, Phys. Rev. B **60**, 13396 (1999).
[32]T. Stopa, S. Kaprzyk, and J. Tobola, J. Phys. Condens. Matter **16**, 4921 (2004).
[33]B. Wiendlocha, PhD thesis, Faculty of Physics and Applied Computer Science, AGH University of Science and Technology, Cracow, Poland (2009).
[34]J. P. Perdew and Y. Wang, Phys. Rev. B **45**, 13244 (1992).
[35]M. I. Aroyo, J. M. Perez-Mato, C. Capillas, E. Kroumova, S. Ivantchev, G. Madariaga, A. Kirov, and H. Wondratschek, Zeit. fur Kryst. **221**, 15 (2006).
[36]M. I. Aroyo, A. Kirov, C. Capillas, J. M. Perez-Mato, and H. Wondratschek, Acta Crystallogr. Sect. A **62**, 115 (2006).
[37]N. D. Mermin and H. Wagner, Phys. Rev. Lett. **17**, 1133 (1966).
[38]P. Gambardella, A. Dallmeyer, K. Maiti, M. C. Malagoli, W. Eberhardt, K. Kern, and C. Carbone, Nature (London) **416**, 301 (2002).
[39]V. Hardy, S. Lambert, M. R. Lees, and D. McK. Paul, Phys. Rev. B **68**, 014424 (2003).
[40]J. Sugiyama, H. Nozaki, Y. Ikedo, K. Mukai, D. Andreica, A. Amato, J. H. Brewer, E. J. Ansaldo, G. D. Morris, T. Takami *et al.*, Phys. Rev. Lett. **96**, 197206 (2006).
[41]V. Pardo, P. Blaha, M. Iglesias, K. Schwarz, D. Baldomir, and J. E. Arias, Phys. Rev. B **70**, 144422 (2004).
[42]I. I. Mazin, D. J. Singh, and A. Aguayo, in *Proceedings of the NATO ARW on Physics of Spin in Solids: Materials, Methods and Applications*, edited by S. Halilov (Kluwer, Dordrecht, 2003), e-print arXiv:cond-mat/0401563.
[43]I. I. Mazin and D. J. Singh, Phys. Rev. B **69**, 020402 (2004).
[44]A. Aguayo and D. J. Singh, Phys. Rev. B **66**, 020401 (2002).
[45]B. Wiendlocha, J. Tobola, and S. Kaprzyk, Phys. Rev. B **73**, 134522 (2006).
[46]A. Aguayo, I. I. Mazin, and D. J. Singh, Phys. Rev. Lett. **92**, 147201 (2004).
[47]R. G. Oraltay, J. J. M. Franse, P. E. Brommer, and A. Menovsky, J. Phys. F **14**, 737 (1984).
[48]W. Cheng, G. Creuzet, P. Garoche, I. A. Campbell, and E. Gratz, J. Phys. F **12**, 475 (1982).
[49]W. L. McMillan, Phys. Rev. **167**, 331 (1968).
[50]J. M. Daams, B. Mitrović, and J. P. Carbotte, Phys. Rev. Lett. **46**, 65 (1981).
[51]B. Wiendlocha, J. Tobola, M. Sternik, S. Kaprzyk, K. Parlinski, and A. M. Oleś, Phys. Rev. B **78**, 060507 (2008).
[52]K. Ikeda and K. A. Gschneidner, J. Magn. Magn. Mater. **30**, 273 (1983).
[53]K. Ikeda and K. A. Gschneidner, J. Magn. Magn. Mater. **31**, 277 (1983).
[54]W. A. Grosshans and W. B. Holzapfel, Phys. Rev. B **45**, 5171 (1992).
[55]C. S. Yoo, H. Cynn, P. Söderlind, and V. Iota, Phys. Rev. Lett. **84**, 4132 (2000).